Monte Carlo Simulations Corroborate PET-Measured Discrepancies in Activity Assessments of Commercial ^{90}Y Vials

Lucrezia Auditore*[1,2], Daniele Pistone*[1,2], Antonio Italiano[2,3], Ernesto Amato[1,2,4], and Silvano Gnesin[5]

[1]*Department of Biomedical and Dental Sciences and of Morphofunctional Imaging, University of Messina, Messina, Italy;* [2]*National Institute for Nuclear Physics, Catania, Italy;* [3]*Department of Mathematical and Computer Science, Physical Sciences, and Earth Sciences, University of Messina, Messina, Italy;* [4]*Health Physics Unit, University Hospital "Gaetano Martino," Messina, Italy; and* [5]*Institute of Radiation Physics, Lausanne University Hospital and University of Lausanne, Lausanne, Switzerland*

In a recent multicenter study, discrepancies between PET/CT-measured activity and vendor-calibrated activity for ^{90}Y glass and resin microspheres were found. In the present work, the origin of these discrepancies was investigated by Monte Carlo (MC) simulations. **Methods:** Three vial configurations, containing ^{90}Y-chloride, ^{90}Y-labeled glass microspheres, and ^{90}Y-labeled resin microspheres, were modeled with GAMOS, and the electric signal generated in an activity meter was simulated. Energy deposition was scored in the activity meter–active regions and converted into electric current per unit activity. Internal bremsstrahlung (IB) photons, always accompanying β-decay, were simulated in addition to ^{90}Y decays. The electric current per source activity obtained for ^{90}Y glass and resin microspheres, I_{glass} and I_{resin}, was compared in terms of relative percentage difference with that of ^{90}Y-chloride (ε_{glass} and ε_{resin}) and each other (δ). The findings of this work were compared with the ones obtained through PET measurements in the multicenter study. **Results:** With the inclusion of IB photons as primary particles in MC simulations, the ε_{glass} and ε_{resin} results were 24.6% ± 3.9% and −15.0% ± 2.2%, respectively, whereas δ was 46.5% ± 1.9%, in very good agreement with the values reported in the multicenter study. **Conclusion:** The MC simulations performed in this study indicate that the discrepancies recently found between PET/CT-measured activity and vendor-calibrated activity for ^{90}Y glass and resin microspheres can be attributed to differences in the geometry of the respective commercial vials and to the metrologic approach adopted for activity meter calibration with a ^{90}Y-chloride liquid source. Furthermore, IB photons were shown to play a relevant role in determining the electric current in the activity meter.

Key Words: Monte Carlo; resin and glass microspheres; ^{90}Y; internal bremsstrahlung

J Nucl Med 2023; 64:1471–1477
DOI: 10.2967/jnumed.123.265494

The use of ^{90}Y for radionuclide therapy in nuclear medicine considers a variety of therapeutic options: radiosynoviorthesis (*1*), anti-CD20 antibodies (*2*), radiolabeled peptides (*3*), and selective internal radiotherapy with glass and resin ^{90}Y-labeled microspheres (*4*).

In particular, ^{90}Y transarterial radioembolization by permanent implantation of ^{90}Y-labeled microspheres is an established therapeutic option for unresectable primary hepatic carcinoma and liver metastases (*4–6*). Selective internal radiotherapy has been applied for 2 decades, and hundreds of thousands of patients have benefited from this treatment so far, worldwide. Clear evidence of the superiority of dosimetry-based treatment personalization is present in the literature (*7*); hence, treatment personalization of the administered therapeutic activity, based on predictive dosimetry, is now broadly recommended.

An accurate determination of the therapeutic administered activity is key in dose–response studies aiming at optimization of treatment safety and efficacy and in view of possible combined internal and external irradiator therapeutic scenarios (*8–10*). Presently, a quantitative accuracy within 10% is considered the minimum standard for assessment of a therapeutic activity administration (*11*).

Evidence of possible discrepancies from the vendor-declared calibrated activity was found for the resin spheres (*12*). Recently, Gnesin et al. (*13*), in a multicenter and multidevice investigation, reported significant discrepancies between PET/CT-measured activity and vendor-calibrated activity for both ^{90}Y microsphere devices. Furthermore, ^{90}Y activities assessed with PET measurements were found to systematically underestimate the vendor-calibrated activity for glass spheres (−21% on average) and overestimate for the resins (+15%). The relative activity difference between resin and glass microspheres averages 46%. Interestingly, good agreement between PET- and vendor-calibrated activities was found for a set of vials containing a homogeneous ^{90}Y-chloride liquid solution.

A possible explanation for the observed discrepancies could reside in differences in geometric configuration and material composition across the 3 commercial products (^{90}Y-labeled resin and glass microsphere vials and the vial containing ^{90}Y in a homogeneous liquid chloride solution). In this work, we performed Monte Carlo (MC) simulations to model the output signal from a reference activity meter in the 3 commercial ^{90}Y vial configurations. We compared the MC results with the recently published experimental results (*12,13*).

MATERIALS AND METHODS

We hypothesized that the differences in geometric configuration and material composition across the 3 vial configurations potentially lead to an important difference in the emitted bremsstrahlung energy spectrum contributing to the signal generation in activity meters.

Received Jan. 20, 2023; revision accepted Apr. 25, 2023.
For correspondence or reprints, contact Antonio Italiano (antonio.italiano@ct.infn.it) or Ernesto Amato (ernesto.amato@unime.it).
*Contributed equally to this work.
Published online Jul. 13, 2023.

Consequently, activity for glass and resin microsphere vials is misestimated adopting the configuration typically used at the manufacturer site before shipping, where the calibrated vial activity is determined using a liquid ^{90}Y-chloride metrology standard.

To investigate the validity of this hypothesis, we implemented 3 vendor-specific vial geometries and compositions in dedicated MC simulations and compared the findings of this study with experimental results recently published in the literature.

MC Simulations

We simulated measurement of the activity of the 3 radioactive sources and respective vials with a commercial activity meter, using GAMOS 6.2 (*14*), a user-friendly interface of the GEANT4 code (*15–17*) extensively validated in the literature (*18*).

The implementation of the geometries will be detailed in the following subsections.

Concerning the simulated radioactive sources, ^{90}Y is a β-emitter decaying to ^{90}Zr with a half-life of 64.05 h. It has an endpoint energy of 2.28 MeV and an average energy of 0.936 MeV, giving the β-particles a maximum range of approximately 1.1 cm in water (*19*). For the 3 radioactive sources, we used the GEANT4 RadioactiveDecay module, which simulates the ^{90}Y β-decay considering the creation of the chosen isotope and following its decay chain until a stable ion is produced.

As highlighted in our recent papers (*20,21*), GEANT4 RadioactiveDecay does not include internal bremsstrahlung (IB) emission accompanying the β-decay.

Consequently, to account for IB emission, an additional source term emitting photons was considered and photon energy was sampled according to the IB spectrum model validated by Auditore et al. (*21*) (supplemental data section A; supplemental materials are available at http://jnm.snmjournals.org).

Concerning the physics models, GmEMExtendedPhysics, which uses by default the Livermore low-energy electromagnetic interaction models, including atomic deexcitation, was applied (*22*). In each simulation, we ran 10^8 events to obtain results with statistical relative errors of less than 2%. The particle spatial propagation considered a range cutoff of 1 μm. No variance reduction technique was used. Simulations were run on an Intel Core i7 fourth-generation processor; each simulation with ^{90}Y sources required about 6 h, whereas each simulation with IB photons as primary particles required less than 1 h.

Finally, we evaluated the accuracy of the performed MC simulation as a function of the assumed geometry for the vials and the activity meter. To achieve this aim, we varied the thickness of the walls in a range $\pm 3\sigma$ with respect to the mean values used to build the model, where σ is the SD associated with the assumed dimensions.

The Activity Meter

We implemented in the MC simulations the geometry and composition of the activity meter Veenstra, model VDC-405, by Comecer, according to the technical layouts provided by the vendor (*23*). This setup has already been validated in our previous work (*22,24*), and more geometric details are reported in supplemental data section B.

The energy deposition, E_{dep}, in the sensitive volume of the activity meter was scored for all simulated sources and converted into electric current per source activity (pA/MBq), as discussed by Auditore et al. (*21*) and reported in supplemental data section C.

The electric current per source activity obtained for ^{90}Y glass and resin microspheres, I_{glass} and I_{resin}, were compared with that for ^{90}Y-chloride by calculating the relative percentage differences, ε_{glass} and ε_{resin}, as

$$\varepsilon_k(\%) = 100 \cdot \frac{I_k - I_{chloride}}{I_{chloride}}, \qquad \text{Eq. 1}$$

where k stands for glass or resin.

Moreover, I_{glass} was compared with I_{resin}, estimating the relative percentage difference, δ:

$$\delta(\%) = 100 \cdot \frac{I_{glass} - I_{resin}}{I_{resin}}. \qquad \text{Eq. 2}$$

Finally, values of δ obtained in this work were compared with the relative percentage difference between glass and resin microsphere activity calibrations, δ*, obtained by Gnesin et al. (*13*).

^{90}Y-Chloride Source

The ^{90}Y-chloride source was implemented in MC simulations by homogeneously sampling ^{90}Y decaying nuclides in 0.5 mL of water (G4_water, density [d] = 1 g/cm^3) contained in a Pyrex (Corning) vial (G4_Pyrex glass, d = 2.23 g/cm^3) with an aluminum cap (G4_aluminum, d = 2.699 g/cm^3). Dimensions of a ^{90}Y-chloride vial (Curium Pharma) were carefully measured to reproduce the actual vial geometry in the MC simulation as shown in Figure 1A. The concerned vial was 1 of the 2 ^{90}Y-chloride vials measured at Centre Hospitalier Universitaire Vaudois by Gnesin et al. (*13*).

^{90}Y Glass Microsphere Source

Commercially available ^{90}Y glass microspheres consist of insoluble glass microspheres with an average diameter ranging from 15 to 35 μm, as stated on the manufacturer's datasheet (*25*), and an average density of 3.29 g/cm^3, as stated by Paxton et al. (*26*). ^{90}Y is present throughout the volume of the microspheres, conferring to each an activity of about 2,500 Bq. ^{90}Y glass microspheres are available in standard activities ranging from 3 to 20 GBq at calibration, as reported in the manufacturer's manual (*27*). The bottom of the vial containing ^{90}Y glass microspheres in solution with water has a v-shape, and its dimensions have been carefully measured to reproduce the correct geometry in MC simulation as shown in Figure 1B. The vial is made of Pyrex and has an aluminum cap.

In the simulated configuration, the vial is placed in a vertical position inside the activity meter; ^{90}Y glass microspheres deposit on the bottom of the vial, and the volume of the precipitate depends on the number of microspheres inside the solution, which in turn depends on the activity required by the user. The rest of the vial is filled with water, for a total filling volume of 0.8 mL.

The ^{90}Y glass microsphere precipitate was reproduced in MC simulation as a glass matrix made of Y_2O_3 (user-defined Y_2O_3, d = 5.01 g/cm^3), aluminum oxide (G4_aluminum oxide, d = 3.97 g/cm^3), and silicon dioxide (G4_silicon dioxide, d = 2.32 g/cm^3) in the proportion 40% Y_2O_3 to 20% Al_2O_3 to 40% SiO_2 (percentages by weight) (*28*) with interstitial water. Primary particles (^{90}Y and IB photons) were sampled uniformly throughout the glass matrix.

The volume and density of the ^{90}Y glass precipitate, V_{prec} and ρ_{prec}, were calculated taking into account random close packing for hard spheres (*29*), as reported in supplemental data section D.

For this study, an activity of 3 GBq was chosen, corresponding to 1.2 million microspheres in the vial; the ^{90}Y glass microsphere precipitate, made of 85.09% glass matrix and 14.91% water (percentages by weight), with a density of 2.45 g/cm^3, has a volume of $1.55 \cdot 10^{-2}$ cm^3.

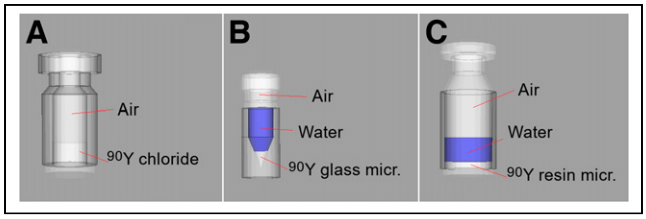

FIGURE 1. Three-dimensional view of ^{90}Y-chloride (A), ^{90}Y glass (B) and ^{90}Y (C) resin microspheres, as simulated with GAMOS.

Nevertheless, to verify the robustness of this study on the considered activity, and consequently on the volume occupied by the ^{90}Y glass microspheres, additional simulations were performed for the commercially available activities listed in Table 1.

^{90}Y Resin Microsphere Source

^{90}Y resin microspheres consist of insoluble resin microspheres with a mean diameter of 32 ± 10 μm and a density of 1.125–1.6 g/cm^3 (*30*). ^{90}Y is affixed to the resin microspheres via an ion exchange process and is present only on the surface of the microspheres. Each vial contains 5 mL of solution with 3 GBq of ^{90}Y and 44 (±2.6) million resin microspheres (*30*) that deposit at the bottom. The dimensions of the vial were carefully measured to reproduce the correct vial geometry in the MC simulation, as shown in Figure 1C. The vial is made of Pyrex and has an aluminum cap.

The ^{90}Y resin microsphere precipitate was reproduced in MC simulation as a polystyrene matrix (G4_polystyrene, d = 1.06 g/cm^3) with interstitial water. Primary particles (^{90}Y and IB photons) were sampled uniformly throughout the resin matrix.

The volume and density of the precipitate were calculated as for ^{90}Y glass microspheres (supplemental data section D). For 3 GBq of activity, the volume of the precipitate was 1.19 cm^3, and it was made of 73.49% polystyrene matrix and 26.51% water (percentages by weight), with a density of 1.38 g/cm^3.

Scoring of Photons Emitted by Sources

Besides the energy deposition in the active volume of the activity meter, to better understand the obtained results, we scored the energy distribution of photons escaping the vial and contributing to the signal generated in the activity meter. To this aim, the World volume and the detector were set to the material G4_galactic (empty space) and the photons were scored at the inner cylindric surface of the activity meter, classifying them according to their energy. The estimated photon spectra for ^{90}Y-chloride, ^{90}Y glass microspheres, and ^{90}Y resin microspheres were then compared with each other.

Comparison with PET Measurements from Literature

Assuming that at the manufacturer's site the activity meter calibration factor, c^M, is obtained with a standard ^{90}Y-chloride solution and then used to measure the activity of ^{90}Y sources in different vial configurations, the manufacturer activity A_x^M is calculated as

$$A_x^M = c^M \cdot i_x, \qquad \text{Eq. 3}$$

where x stands for glass, chloride, or resin and i is the current measured by the activity meter.

In this approach, c^M is assumed to be the same for resin, chloride, and glass solutions.

In this study, we hypothesized—also in light of the results reported by Gnesin et al. (*13*)—that the actual calibration factors, c_x, depend on the vial geometry and on the source configuration; consequently, the activities should be calculated using the proper calculation factor:

$$A_x = c_x \cdot i_x, \qquad \text{Eq. 4}$$

where A_x is the actual activity.

TABLE 1
^{90}Y Glass Microspheres Activities Considered for Robustness Analysis

Activity (GBq)	Microspheres (n)	V_{prec} (cm^3)
10.0	$4.0 \cdot 10^6$	$5.16 \cdot 10^{-2}$
16.5	$6.6 \cdot 10^6$	$8.52 \cdot 10^{-2}$
20.0	$8.0 \cdot 10^6$	$10.3 \cdot 10^{-2}$

Gnesin et al. measured the A^{PET}/A^M ratios for ^{90}Y glass and resin microspheres and ^{90}Y-chloride solution. Assuming A^{PET} as the actual activity, A_x, we can express the measured ratios as

$$\frac{A_x^{PET}}{A_x^M} = \frac{A_x}{A_x^M} = \frac{c_x \cdot i_x}{c^M \cdot i_x} = \frac{c_x}{c^M}, \qquad \text{Eq. 5}$$

And then the A^{PET}/A^M ratios measured by Gnesin et al. would reflect the difference between the used and the actual calibration factors. It should be stressed that A^{PET}/A^M was found by Gnesin et al. to be equal to 1 for chloride vials, experimentally confirming that the manufacturer standard is chloride solution and thus that $A^M = A_{chloride}$.

In this study, we estimate, by MC simulation, $I_x = i_x/A_x$, which, from Equation 4, results in

$$I_x = \frac{i_x}{A_x} = \frac{1}{c_x}. \qquad \text{Eq. 6}$$

Using Equation 6 in Equation 5, we obtain

$$\frac{A_x^{PET}}{A_x^M} = \frac{1}{c^M \cdot I_x}. \qquad \text{Eq. 7}$$

Referring to ^{90}Y-chloride solution as a common metrologic reference ($c^M = c_{chloride}$) and assuming the same amount of activity for each vendor vial ($A^M_{chloride} = A^M_{glass} = A^M_{resin}$), it follows that

$$\frac{A_{glass}^{PET}}{A_{chloride}^{PET}} = \frac{I_{chloride}}{I_{glass}} \qquad \text{Eq. 8}$$

$$\frac{A_{resin}^{PET}}{A_{chloride}^{PET}} = \frac{I_{chloride}}{I_{resin}}, \qquad \text{Eq. 9}$$

Therefore, electric current ratios obtained from MC simulations can be directly compared with the PET-derived activity ratios reported by Gnesin et al. (*13*).

RESULTS

In Table 2 and Figure 2, we reported the MC estimates obtained in terms of electric current per unit activity (sampling only ^{90}Y as the primary source, without IB). A ^{90}Y glass microsphere vial gives an electric signal 30.7% higher than ^{90}Y-chloride, whereas a signal 17.2% lower is obtained for a ^{90}Y resin microsphere vial (Fig. 2B); these values are in fair agreement with the differences found by Gnesin et al. (*13*) of 27% and −13% between activities measured with PET and by the glass and resin microsphere manufacturers. The relative difference between ^{90}Y glass and resin microspheres is 57.8% ± 2.4%, a value higher than the one reported by Gnesin et al. (*13*).

To obtain more accurate estimates, and in light of the relevance of IB emission pointed out in our recent studies (*20,21*), MC simulation was performed also including IB photons, γ_{IB}, as an additional source term, and the results are reported in Table 3 and shown in Figure 2C. Simulating ^{90}Y and IB photons as primary particles, we found that the differences between the electric current per unit activity for ^{90}Y glass and resin microspheres and for ^{90}Y-chloride reduces to 24.6% ± 3.9% and −15.0% ± 2.2% (Fig. 2D), thus improving agreement with the measurements from Gnesin et al. (*13*). Also the relative percentage difference between ^{90}Y glass and resin microspheres reduces to 46.5% ± 1.9%, in very good agreement with the values reported by Gnesin et al. (*13*).

Table 4 reports the ratios of the current per unit activity of chloride versus glass and chloride versus resin configurations, obtained with MC simulations including IB contribution. These values are

TABLE 2
Electric Current per Unit Activity Estimated for ^{90}Y-Chloride, ^{90}Y Glass Microspheres, and ^{90}Y Resin Microspheres, Sampling ^{90}Y as Primary Particle (β-Decay)

Primary particle	$I_{chloride}$ (pA/MBq)	I_{glass} (pA/MBq)	ε_{glass} (%)	I_{resin} (pA/MBq)	ε_{resin} (%)	δ (%)	δ* (%)
^{90}Y	0.163 ± 0.01	0.213 ± 0.010	30.7 ± 5.2	0.135 ± 0.010	−17.2 ± 2.5	57.8 ± 2.4	46.00 ± 0.15

For comparison, δ* value calculated by method of Gnesin et al. (*13*) is also reported.

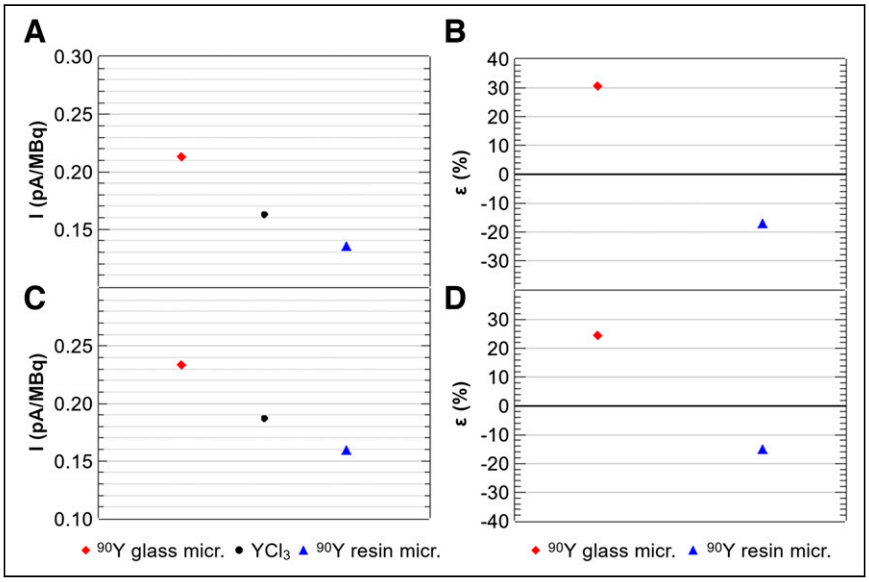

FIGURE 2. (A and C) Electric currents per unit activity estimated from sampling standard ^{90}Y β-decay spectrum (A) or ^{90}Y β-decay with addition of IB photons (C). (B and D) Relative percentage differences, ε_{glass} and ε_{resin}, calculated for MC results without (B) and with (D) IB photons.

in excellent agreement with the activity ratios found by Gnesin et al. (*13*), confirming the assumptions behind Equations 8 and 9.

The geometry used in MC simulations was varied to evaluate the robustness of the model, with respect to the variability in the dimensions of the activimeter and vial geometry. For the applied geometry variations to the activity meter, within the range ±3σ, ε_{glass} resulted in a CI of ±12.6%, an ε_{resin} of ±10.2%, and a δ of ±2.2%.

The modification of the vial dimensions leads to variations of about ±9.4% and ±10.7% for ε_{glass} and ε_{resin}, respectively, and ±2.8% for δ.

When the activity meter and vial geometry variations were combined, the CIs for ε_{glass}, ε_{resin}, and δ were estimated to be ±15.9%, ±14.9%, and ±4.1%, respectively.

The activity of the vial containing ^{90}Y glass microspheres depends as much on the number of microspheres as on the volume occupied by them (Table 1). To test the robustness of this study as a function of the considered ^{90}Y glass microsphere activity, the electric currents per unit activity obtained for the activities listed in Table 1 are reported in Table 5 for comparison purposes. Taking the 3-GBq activity source as the reference, the relative percentage difference between the results is lower than 1%, thus indicating the independence of the MC estimates from the source activity and the robustness of the study in the considered range.

The photon spectra scored at the inner surface of the activity meter are reported in Figure 3. The energy peak at 1,760 keV results from the deexcitation of an excited state of ^{40}Zr to which ^{90}Y decays (*19*). Due to the shape and thickness of the vial, particularly in the v-shaped bottom, the photon yield estimated for the ^{90}Y glass microsphere vial is higher than the yields resulting from ^{90}Y-chloride and ^{90}Y resin microspheres, the latter providing the lowest photon yield. The relevant differences in the energy range 0–1 MeV (Fig. 3B) are reflected in the different electric currents generated in the activity meter for the 3 source vials.

DISCUSSION

In this work, we performed MC simulations of the activity meter signal generation from ^{90}Y sources in 3 commercial vial configurations. We simulated the ^{90}Y decay generating the external bremsstrahlung photons due to the interaction of the β-particles with the surrounding material; in addition, we included the IB photons that

TABLE 3
Electric Current per Unit Activity Estimated for Considered Sources, with Additional Sampling of IB Photons, γ_{IB}, as Primary Particles

Primary particle	$I_{chloride}$ (pA/MBq)	I_{glass} (pA/MBq)	ε_{glass} (%)	I_{resin} (pA/MBq)	ε_{resin} (%)	δ (%)	δ* (%)
γ_{IB}	0.024 ± 0.001	0.020 ± 0.001	−16.7 ± 5.5	0.024 ± 0.001	0.0 ± 0.0*	−16.7 ± 5.5	—
^{90}Y + γ_{IB}	0.187 ± 0.015	0.233 ± 0.012	24.6 ± 3.9	0.159 ± 0.009	−15.0 ± 2.2	46.5 ± 1.9	46.00 ± 0.15

*Within considered significant digits.

Estimates accounting for ^{90}Y decays plus γ_{IB} are also reported. For comparison, δ* value estimated by method of Gnesin et al. (*13*) is also displayed.

TABLE 4
Ratios Between Activities of Glass and Resin Microspheres and ^{90}Y-Chloride Vials

$\frac{A^{PET}_{glass}}{A^{PET}_{chloride}}$	$\frac{I_{chloride}}{I_{glass}}$	$\frac{A^{PET}_{resin}}{A^{PET}_{chloride}}$	$\frac{I_{chloride}}{I_{resin}}$
0.79 ± 0.04	0.80 ± 0.03	1.15 ± 0.06	1.18 ± 0.03

Experimentally obtained by Gnesin et al. (*13*) with PET, compared with ratios of current per unit activity obtained in this study with MC simulations (Eqs. 8 and 9).

originate from the interaction of the emitted β-particles with the electromagnetic field of the emitting nucleus.

We calculated the electric signal produced in the 3 source configurations and computed the relative percentage difference comparing the 2 types of ^{90}Y-labeled microspheres with the ^{90}Y-chloride solution. Moreover, we assessed the relative percentage difference between the electric signal obtained from the glass and resin microspheres.

Taking into account also the IB contribution, we found that for a matched activity of ^{90}Y, the electric signals generated by the ^{90}Y-labeled glass and resin microsphere vials were 24.6% higher and 15.0% lower, respectively, than the signal produced by the vial containing a homogeneous ^{90}Y-chloride solution. Hence, we found a relative difference of 46.5% ± 1.9% for the electric signal estimated for the glass versus resin commercial vials.

We compared the findings of this study with the experimental results recently reported by Gnesin et al. (*13*). We found remarkably good agreement between the relative percentage differences in the electric signal produced by resin versus glass microspheres obtained with MC simulation and the relative percentage difference in total vial activity measured in a ^{90}Y PET/CT experimental setup (*13*). Consequently, equally good agreement was found comparing the ratios of chloride versus glass and chloride versus resin electric signals with the corresponding ratios of activity measured in PET/CT, as detailed in Equations 8 and 9.

Therefore, the measured discrepancies in the activity assessment from commercial vials could be reasonably ascribed to the differences in the geometry and source composition across the 3 vials considered in the study.

PET measurements rely on the detection of coincidence annihilation photons and are, in principle, not sensitive to possible difference

TABLE 5
Electric Currents per Unit Activity Obtained for Different Activities of ^{90}Y Glass Microsphere Source

Activity (GBq)	I_{glass} (pA/MBq)	Relative difference (%)
3	0.233	—
10	0.233	0.0
16.5	0.232	−0.43
20	0.232	−0.43

Relative percentage difference has been calculated with respect to reference activity of 3 GBq in source.

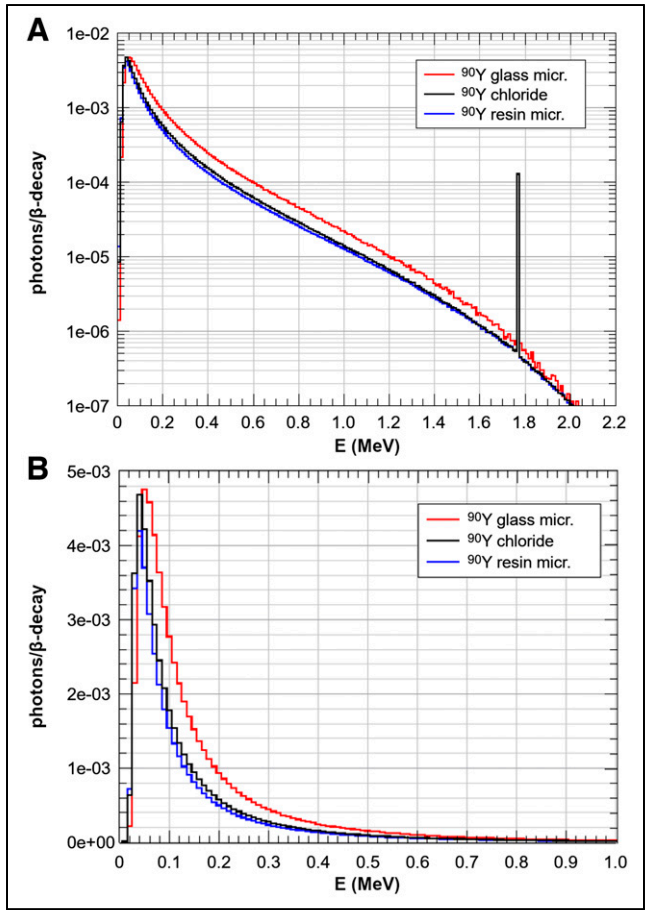

FIGURE 3. (A) Photon spectra sampled at inner surface of activity meter. (B) Zoomed 0- to 1-MeV energy range with linear *y* scale. Primary particles sampled were ^{90}Y and IB photons, γ_{IB}.

in the bremsstrahlung energy spectrum emitted by the different commercial products. Interestingly, Gnesin et al. (*13*) found the best agreement of PET-assessed activity with the vendor-declared calibrated activity for the ^{90}Y-chloride vials. This finding can be explained if we assume that commercial activity meters (with the inclusion of activity meters used by the ^{90}Y manufacturers) rely on a metrologic standard using a ^{90}Y homogeneous liquid compound. Conversely, activity assessments of resin and glass microspheres, characterized by vial geometry and source composition sensibly different from the metrologic ^{90}Y liquid standard, are prone to provide a potentially inaccurate activity evaluation if measured in a device calibrated with a ^{90}Y liquid standard.

Assuming a common metrologic standard related to ^{90}Y liquid chloride solution, as done in Equation 3, glass and resin vial activity assessments from the manufacturer activity meters would result in a systematic overestimation and underestimation, respectively, of the actual ones. Consequently, the glass and resin manufacturers filled their own vials with a lower and higher amount, respectively, of activity than the intended ones. This suggests that product-specific calibration factors should be adopted for each vial configuration.

Furthermore, the results presented by Gnesin et al. (*13*) were best reproduced when considering the IB in addition to the standard ^{90}Y decay spectrum. This aspect can be understood considering that the electric signal generated in the activity meter results

from interactions of all photons that deposit energy—indeed, both internal and external bremsstrahlung photons.

To our knowledge, this is the first study providing a reasonable explanation for the measured disagreement in the total ^{90}Y activity obtained in PET/CT (in a multicenter and multidevice study) when compared with calibrated activity information provided by vendors (*13*).

In addition, we tested the robustness of the results by varying the geometric dimensions of both the activimeter and the vials. Estimations of ε_{glass} and ε_{resin} were found to vary within 16% (±15.9% and ±14.9%, respectively). The relative percentage difference between glass and resin microsphere activity calibrations, δ, shows a CI of ±4.1%, indicating that the considered geometric variations mildly influenced this parameter.

The estimate of 46.5% ± 1.9% for δ must be compared with the experimental δ* obtained from data reported by Gnesin et al. (*13*), who found δ* to equal 46.00% without any direct indication of the CI. From data published in Gnesin et al. (*13*), A^{PET}/A^{M} (resin) = 1.15 ± 0.06 and A^{PET}/A^{M} (glass) = 0.79 ± 0.04, and the CI can be estimated as follows:

$$\frac{\left(\frac{A^{PET}}{A^{M}}\right)_{resin}+SD}{\left(\frac{A^{PET}}{A^{M}}\right)_{glass}-SD}=\frac{(1.15+0.06)}{(0.79-0.04)}=1.61$$

$$\frac{\left(\frac{A^{PET}}{A^{M}}\right)_{rein}-SD}{\left(\frac{A^{PET}}{A^{M}}\right)_{glass}+SD}=\frac{(1.15-0.06)}{(0.79+0.04)}=1.31.$$

Consequently, δ*upper = 61% and δ*lower = 31% and a CI can be assigned to δ* as 46% ± 15%. The MC-estimated δ reproduces the centroid of the gaussian distribution of the experimental δ* and is fully included in its CI (46.5% ± 1.9% vs. 46.00% ± 15%).

Another factor influencing the accuracy of the obtained results concerns the IB spectral distribution used in this study; it was obtained according to the fit of the IB spectrum measurements available in the literature, as reported in our previous work in which we identified the most appropriate model for the ^{90}Y IB spectrum after comparing radiometric measurements and MC simulations (*21,24*); nevertheless, in perspective, new ^{90}Y IB spectrum measurements could help to further refine the model.

CONCLUSION

The MC simulations of the response of a commercial activity meter to sources of ^{90}Y-chloride, ^{90}Y resin microspheres, and ^{90}Y glass microspheres indicate that the discrepancies recently found between PET/CT-measured activity and vendor-calibrated activity for ^{90}Y glass and resin microsphere vials are attributable to the difference in the geometry of the commercial vials, the specific spatial distribution of microspheres in solution or precipitate inside the vial, and the metrologic reference adopted for the activity meter calibration. Finally, the inclusion of IB photons in MC simulations dealing with the ^{90}Y source is advisable because it plays a relevant role in determining the activity meter output.

DISCLOSURE

No potential conflict of interest relevant to this article was reported.

KEY POINTS

QUESTION: What is a possible explanation for the experimentally observed discrepancies between ^{90}Y vial manufacturer-calibrated activities and independent PET quantitative assessment?

PERTINENT FINDINGS: Considering a well counter configuration typical of commercial activity meters, we used MC simulations to assess the electric signal generation for the measurement of commercial vials containing ^{90}Y-labeled glass and resin microspheres and ^{90}Y-chloride in liquid solution. For the same vial activity, simulation gave a relative electric current difference of +24.6% for glass vials and −15% for resin vials as compared with the ^{90}Y liquid chloride solution.

IMPLICATIONS FOR PATIENT CARE: Accurate activity assessment is mandatory for therapeutic procedures and key for the establishment of reliable dose–effect studies.

REFERENCES

1. Torres Berdeguez MB, Mirta B, Thomas S, et al. Dosimetry in radiosynoviorthesis: ^{90}Y VS. ^{153}Sm. *Health Phys.* 2018;114:1–6.
2. Ma D, McDevitt M, Barendswaard E, et al. Radioimmunotherapy for model B cell malignancies using ^{90}Y-labeled anti-CD19 and anti-CD20 monoclonal antibodies. *Leukemia.* 2002;16:60–66.
3. Menda Y, Madsen MT, O'Dorisio TM, et al. ^{90}Y-DOTATOC dosimetry–based personalized peptide receptor radionuclide therapy. *J Nucl Med.* 2018;59:1692–1698.
4. Levillain H, Bagni O, Deroose CM, et al. International recommendations for personalised selective internal radiation therapy of primary and metastatic liver diseases with yttrium-90 resin microspheres. *Eur J Nucl Med Mol Imaging.* 2021;48:1570–1584.
5. Chiesa C, Sjogreen-Gleisner K, Walrand S, et al. EANM dosimetry committee series on standard operational procedures: a unified methodology for ^{99m}Tc-MAA pre- and ^{90}Y peri-therapy dosimetry in liver radioembolization with ^{90}Y microspheres. *EJNMMI Phys.* 2021;8:77.
6. Weber M, Lam M, Chiesa C, et al. EANM procedure guideline for the treatment of liver cancer and liver metastases with intra-arterial radioactive compounds. *Eur J Nucl Med Mol Imaging.* 2022;49:1682–1699.
7. Garin E, Tselikas L, Guiu B, et al. Personalised versus standard dosimetry approach of selective internal radiation therapy in patients with locally advanced hepatocellular carcinoma (DOSISPHERE-01): a randomised, multicentre, open-label phase 2 trial. *Lancet Gastroenterol Hepatol.* 2021;6:17–29.
8. Lam MG, Abdelmaksoud MH, Chang DT, et al. Safety of ^{90}Y radioembolization in patients who have undergone previous external beam radiation therapy. *Int J Radiat Oncol Biol Phys.* 2013;87:323–329.
9. Cremonesi M, Ferrari M, Botta F, et al. Planning combined treatments of external beam radiation therapy and molecular radiotherapy. *Cancer Biother Radiopharm.* 2014;29:227–237.
10. Wang TH, Huang PI, Hu YW, et al. Combined yttrium-90 microsphere selective internal radiation therapy and external beam radiotherapy in patients with hepatocellular carcinoma: from clinical aspects to dosimetry. *PLoS One.* 2018;13:e0190098.
11. Konijnenberg M, Herrmann K, Kobe C, et al. EANM position paper on article 56 of the council directive 2013/59/Euratom (basic safety standards) for nuclear medicine therapy. *Eur J Nucl Med Mol Imaging.* 2021;48:67–72.
12. Graves SA, Martin M, Tiwari A, Merrick MJ, Sunderland JJ. SIR-Spheres activity measurements reveal systematic miscalibration. *J Nucl Med.* 2022;63:1131–1135.
13. Gnesin S, Mikell JK, Conti M, et al. A multicenter study on observed discrepancies between vendor-stated and PET-measured ^{90}Y activities for both glass and resin microsphere devices. *J Nucl Med.* November 23, 2022 [Epub ahead of print].
14. Arce P, Rato P, Cañadas M, Lagares JI. GAMOS: a GEANT4-based easy and flexible framework for nuclear medicine applications. *IEEE Nucl Sci Symp Conf Rec.* 2008:3162–3168.
15. Agostinelli S, Allison J, Amako K, et al. Geant4: a simulation toolkit. *Nucl Instrum Methods Phys Res A.* 2003;506:250–303.

16. Allison J, Amako K, Apostolakis J, et al. Geant4 developments and applications. *IEEE Trans Nucl Sci.* 2006;53:270–278.
17. Allison J, Amako K, Apostolakis J, et al. Recent developments in Geant4. *Nucl Instrum Methods Phys Res A.* 2016;835:186–225.
18. Arce P, Lagares JI, Harkness L, et al. Gamos: a framework to do Geant4 simulations in different physics fields with an user-friendly interface. *Nucl Instrum Methods Phys Res A.* 2014;735:304–313.
19. Nuclear data services. International Atomic Energy Agency website. https://www-nds.iaea.org/. Accessed June 22, 2023.
20. Italiano A, Auditore L, Amato E. Enhancement of radiation exposure risk from β-emitter radionuclides due to internal Bremsstrahlung effect: a Monte Carlo study of ^{90}Y case. *Phys Med.* 2020;76:159–165.
21. Auditore L, Juget F, Italiano A, et al. Experimental evidence of internal Bremsstrahlung photons from ^{90}Y decay. *Phys Med.* 2021;90:158–163.
22. GAMOS user guide. GAMOS website. http://fismed.ciemat.es/GAMOS/gamos_userguide.php. Accessed June 22, 2023.
23. IBC dose calibrator. Comecer website. https://www.comecer.com/ibc-dose-calibrator/. Accessed June 22, 2023.
24. Auditore L, Juget F, Pistone D, Nedjadi Y, Amato E, Italiano A. Internal Bremsstrahlung emission during ^{32}P decay. *Radiat Meas.* 2022;155:106799.
25. TheraSphere™ Y90 glass microspheres. Boston Scientific website. https://www.bostonscientific.com/en-EU/products/selective-internal-radiation-therapy/therasphere-y90-glass-microspheres.html. Accessed June 22, 2023.
26. Paxton AB, Davis SD, DeWerd LA. Determining the effects of microsphere and surrounding material composition on ^{90}Y dose kernels using EGSNRC and MCNP5. *Med Phys.* 2012;39:1424–1434.
27. Instructions for use: TheraSphere™ yttrium-90 glass microspheres. Boston Scientific website. https://www.bostonscientific.com/content/dam/elabeling/pi/OTT-00221_Rev1_TheraSphere_en_s.pdf. Updated March 2021. Accessed June 22, 2023.
28. Baino F, Fiume E, Ciavattini S, et al. Biomedical radioactive glasses for brachytherapy. *Materials (Basel).* 2021;14:1131.
29. Song C, Wang P, Makse H. A phase diagram for jammed matter. *Nature.* 2008;453:629–632.
30. SIR-Spheres® Y-90 resin microspheres. Sirtex website. https://www.sirtex.com/ap/products/sir-spheres-y-90-resin-microspheres/about-sir-spheres/. Accessed June 22, 2023.